Pergamon

Int. J. Heat Mass Transfer. Vol. 40, No. 17, pp. 4061–4071, 1997

Printed in Great Britain
0017–9310/97 $17.00+0.00

PII: S0017–9310(97)00061–6

Double diffusive natural convection in a square enclosure with heat and mass diffusive walls

V. A. F. COSTA

Departamento de Engenharia Mecânica da Universidade de Aveiro, Campus Universitário de Santiago, 3810 Aveiro, Portugal

(*Received* 14 *October* 1996 *and in final form* 7 *February* 1997)

Abstract—Double diffusive steady natural convection in a vertical stack of square enclosures, with heat and mass diffusive walls, is studied numerically. The main objectives of the paper are the statement of the complete mathematical model for this kind of problem, and the presentation and analysis of some significant results showing the influence of the heat and mass transfer participating walls. The analysis is concentrated on a restricted set of numerical results, obtained from a limited set of particular combinations of the governing dimensionless parameters for a cavity filled with moist air. The heat and mass transfer characteristics of the vertical stack are analysed through the heat and masslines, and the local and global Nusselt and Sherwood numbers over all the walls of the cavity. © 1997 Elsevier Science Ltd.

1. INTRODUCTION

Double diffusive natural convection in enclosures is a problem studied to some extent both numerically and experimentally. Some recent studies include the experimental work of Kamotani *et al.* [1], the mixed experimental/numerical works of Kamakura and Ozoe [2] and Wee *et al.* [3], and the numerical work of Béghein *et al.* [4]. There are also some recent works concerning similarity analysis devoted to the boundary layer regime [5, 6], including even more recently a mixed similarity/numerical treatment. The main objectives of such works are usually the analysis of the resulting flow structure, and the heat and mass transfer parameters as functions of the nondimensional parameters governing the involved phenomena. There is also a set of recent works devoted to the double diffusive natural convection in enclosures filled with a porous material, see for example Refs. [7, 8].

To the author's knowledge, there are no published results that, in search of the aforementioned global objectives, include the effects of heat and mass transfer through walls in both crossing and axial directions. This is true for a single cavity, and also for a vertical stack of heat and mass transfer communicating cavities. For the situation of single convection heat transfer, refer to the works of Kim and Viskanta [9], Du and Bilgen [10], Chung and Trefethen [11] Nishimura *et al.* [12] and Costa *et al.* [13], which include the wall conduction effects over the flow structure and the heat and mass transfer parameters.

Thinking essentially of building construction elements, whose walls are not perfectly impermeable and adiabatic, a more realistic study should include these two effects. Due to the number of dimensionless parameters involved, a contained study can only consider some fewer combinations, with this limited study putting forward the complete mathematical model and the most important expected characteristics of the fluid flow and heat and mass transfer phenomena. As, at the present time, there are numerical techniques and commercial numerical codes available to solve such problems, specific situations can easily be the object of specific treatment in order to obtain their corresponding specific solutions. One powerful characteristic of such practice is that there are no limitations over the values assumed by the governing parameters, which is not the case with experimental and similarity approaches.

It remains to be noted that, in this study, there are problems not considered related with flow instabilities, transition to turbulence, and the condensation phenomenon when the medium that fills a cavity is a gaseous mixture with a condensable component.

2. MATHEMATICAL AND NUMERICAL MODELLING

2.1. *Physical model*

The domain under analysis is, as sketched in Fig. 1, a square, two-dimensional cavity, suffering the influence of a gravitational field, filled with a fluid which contains a pollutant concentration.

The vertical cavity walls are maintained at constant and uniform different levels of temperature and concentration, thus giving rise to a double-diffusive free convective fluid flow. The considered horizontal half walls are of equal thickness, and are assumed to be of the same material with, in the general case, non zero thermal and mass diffusivities.

2.2. *Model assumptions*

The fluid and the pollutant are assumed to be completely mixed, this mixture being the Newton–Fourier

NOMENCLATURE

B	thickness of the separating wall
C	concentration ($C = m_{solutal}/m_{total}$)
c_p	constant pressure specific heat
D	mass diffusivity
g	gravitational acceleration
H	heat function
k	thermal conductivity
L	side length of the cavity
Le	Lewis number
m	mass
M	mass function
M	molecular weight
n	inward normal direction
N	buoyancy ratio ($N = \beta_C \Delta C_{max}/\beta_T \Delta T_{max}$)
Nu	Nusselt number
p	pressure
Pr	Prandtl number
Ra	Rayleigh number
Rc	thermal conductivity ratio
Rd	mass diffusion coefficient ratio
Sc	Schmidt number
Sh	Sherwood number
T	temperature
u, v	velocity components
x, y	Cartesian co-ordinates.

Greek symbols

α	thermal diffusivity
β	volumetric expansion coefficient
ν	kinematic viscosity
ρ	density
ω	specific humidity in a dry basis.

Subscripts

abs	absolute scale
C	referring to mass transfer
f	referring to the fluid
H	higher level
L	lower level
P	at the P point
T	referring to heat transfer
w	separating walls
0	reference value
1	diffusing species
2	non-diffusing species
*	dimensionless.

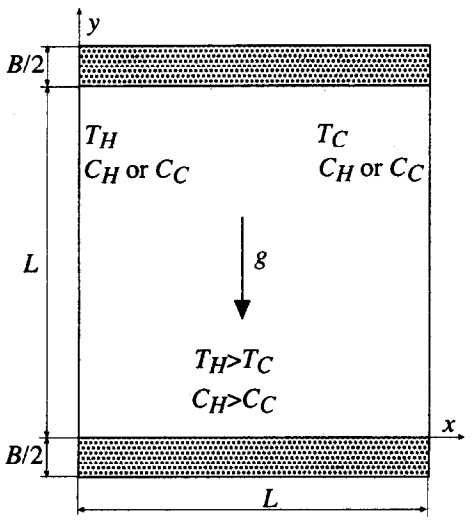

Fig. 1. Physical model and geometry.

fluid that fills the cavity, which flows in laminar conditions and does not experience any phase change. This fluid is assumed to be incompressible but expands or contracts under the action of temperature and/or concentration gradients. This assumption leads to the Boussinesq approximation if both the temperature and concentration difference levels are maintained within certain limits.

The mixture density is assumed to be uniform over all the cavity, except for the buoyancy term, in which the density is taken as a function of both the temperature and concentration fields. Beginning with $\rho = \rho(T, C)$, elementary thermodynamics states that $\beta_T = -(\partial\rho/\partial T)_C/\rho$ is the volumetric thermal expansion coefficient and, similarly, $\beta_C = -(\partial\rho/\partial C)_T/\rho$ is taken as the volumetric mass expansion coefficient. The mixture density can thus be obtained from a given reference value $\rho_0 = \rho(T_0, C_0)$ as [14]

$$\rho = \rho_0[1-\beta_T(T-T_0)-\beta_C(C-C_0)] \qquad (1)$$

assuming that the derivatives and the denominator ρ present in the definitions of β_T and β_C are constant.

The usual situations correspond to a positive β_T, the only frequent exception being the water between 0 and nearly 4°C; in this way, the usual situations can lead to either positive or negative β_C. If the fluid can be considered as a mixture of ideal gases, $\beta_T = 1/T_{abs}$ and $\beta_C = (M_2 - M_1)/[(M_2 - M_1)C + M_1]$, where M_1 is the molecular weight of the diffusing pollutant and M_2 is the molecular weight of the remaining fluid.

When the energy conservation is under analysis, it is assumed that the thermal levels are small and similar enough in order to validate the non-consideration of the thermal radiation between the walls, which encloses a fluid assumed to be radiatively non-participating. The energy terms due to viscous dissipation and change of temperature due to reversible deformation (work of pressure forces) are not considered.

Given the two-component mixture under analysis, the energy terms of interdiffusional convection and diffusion thermo (Dufour effect) are also not considered [15]. Thus, the only considered diffusion term is that due to Fourier conduction.

Analysing the pollutant mass conservation, considered in this work as the ratio between the mass of pollutant to the total mass ($C = m_1/m$), the only considered diffusional term is that due to Fick diffusion. The pressure diffusion, body force diffusion and thermal diffusion (Soret effect) terms are not considered [15]. If the mixture under analysis is moist air, C is the specific humidity in a wet basis, which is related to the specific humidity ω in a dry basis as $C = \omega/(1+\omega)$.

Additionally, all the heat and mass transfer properties of the involved media (two mixture components, the mixture and the solid walls) are assumed to be constant, except for the density appearing in the buoyancy terms, as explained above. It should be noted that, in reality, the properties of the mixture that fills the cavity are dependent on the concentration level of the diffusing species at each point.

2.3. *Model equations*

Introducing the dimensionless variables

$$u_* = uL/\alpha; \quad v_* = vL/\alpha, \tag{2}$$

$$x_* = x/L; \quad y_* = y/L, \tag{3}$$

$$T_* = (T-T_C)/(T_H-T_C); \tag{4}$$

$$C_* = (C-C_C)/(C_H-C_C),$$

$$p_* = (p+\rho_0 g y)/(\rho_0(\alpha/L)^2) \tag{5}$$

where p_* is thus the nondimensional driving pressure, one obtains the following set of partial differential equations:

Continuity equation

$$\frac{\partial u_*}{\partial x_*} + \frac{\partial v_*}{\partial y_*} = 0 \tag{6}$$

x_* momentum equation

$$\frac{\partial}{\partial x_*}(u_* u_*) + \frac{\partial}{\partial y_*}(v_* u_*) = -\frac{\partial p_*}{\partial x_*} + Pr\left(\frac{\partial^2 u_*}{\partial x_*^2} + \frac{\partial^2 u_*}{\partial y_*^2}\right) \tag{7}$$

y_* momentum equation

$$\frac{\partial}{\partial x_*}(u_* v_*) + \frac{\partial}{\partial y_*}(v_* v_*) = -\frac{\partial p_*}{\partial y_*} + Pr\left(\frac{\partial^2 v_*}{\partial x_*^2} + \frac{\partial^2 v_*}{\partial y_*^2}\right) + Ra_T Pr(T_* + NC_*) \tag{8}$$

Energy conservation equation on the fluid

$$\frac{\partial}{\partial x_*}(u_* T_*) + \frac{\partial}{\partial y_*}(v_* T_*) = \left(\frac{\partial^2 T_*}{\partial x_*^2} + \frac{\partial^2 T_*}{\partial y_*^2}\right) \tag{9}$$

Energy conservation equation on the solid walls

$$\frac{\partial^2 T_*}{\partial x_*^2} + \frac{\partial^2 T_*}{\partial y_*^2} = 0 \tag{10}$$

Pollutant mass conservation equation on the fluid

$$\frac{\partial}{\partial x_*}(u_* C_*) + \frac{\partial}{\partial y_*}(v_* C_*) = \frac{1}{Le}\left(\frac{\partial^2 C_*}{\partial x_*^2} + \frac{\partial^2 C_*}{\partial y_*^2}\right) \tag{11}$$

Pollutant mass conservation equation on the solid walls

$$\frac{\partial^2 C_*}{\partial x_*^2} + \frac{\partial^2 C_*}{\partial y_*^2} = 0. \tag{12}$$

From the foregoing equations are emerging the dimensionless parameters

$$Pr = \nu/\alpha, \tag{13}$$

$$Ra_T = g\beta_T L^3 (T_H - T_C)/\nu\alpha, \tag{14}$$

$$N = \beta_C (C_H - C_C)/\beta_T (T_H - T_C), \tag{15}$$

$$Le = \alpha/D. \tag{16}$$

Another parameter than can be introduced is the Schmidt number, $Sc = \nu/D$.

The Prandtl and thermal Rayleigh parameters given by equations (13) and (14), respectively, are usual when analysing the single natural convection heat transfer in enclosures. In this way, the N and Lewis parameters given, respectively, by equations (15) and (16) arise, in addition, when analysing the combined convective heat and mass transfer in enclosures. Parameter N is the buoyancy ratio, which is the ratio between the solutal and thermal buoyancy forces. It can be either positive or negative, its sign depending on that of the ratio between the volumetric expansion coefficients β_T and β_C. Its limits are that it is null for no pollutant diffusion and infinite for no thermal diffusion. One notes that when equations (9) and (11) are subjected to the same boundary conditions, the T_* and C_* fields are coincident for $Le = 1$.

It should be mentioned that a Rayleigh number referring to mass transfer, similar to Ra_T referring to heat transfer as defied by equation (14), can be defined analogously as $Ra_C = g\beta_C L^3 (C_H - C_C)/\nu D$.

2.4. *Boundary conditions*

Over the walls of the cavity we impose

$$u_*(0, y_*) = u_*(1, y_*) = u_*(x_*, 0) = u_*(x_*, 1) = 0, \tag{17}$$

$$v_*(0, y_*) = v_*(1, y_*) = v_*(x_*, 0) = v_*(x_*, 1) = 0. \tag{18}$$

With such boundary conditions, it is assumed that the pollutant mass flow through the walls is small enough in order to validate the use of zero normal velocity values at the walls.

Prescription of T_* and C_* over the vertical walls can lead to a situation of combined or opposed buoyancy effects. Over the vertical walls it is thus prescribed that

$$T_*(0, y_*) = 1; \quad T_*(1, y_*) = 0 \tag{19}$$

$$C_*(0, y_*) = 1; \quad C_*(1, y_*) = 0$$

for combined buoyancy effects, (20a)

or

$$C_*(0, y_*) = 0; \quad C_*(1, y_*) = 1$$

for opposed buoyancy effects. (20b)

The problem under analysis is a conjugate heat and mass transfer problem where it is assumed that, at each interface fluid-horizontal wall of the cavity,

$$-\left(k\frac{\partial T}{\partial y}\right)_f = -\left(k\frac{\partial T}{\partial y}\right)_w, \tag{21}$$

$$-\left(\rho_0 D\frac{\partial C}{\partial y}\right)_f = -\left(\rho D\frac{\partial C}{\partial y}\right)_w \tag{22}$$

or, in a dimensionless form,

$$\left(\frac{\partial T_*}{\partial y_*}\right)_f = Rc\left(\frac{\partial T_*}{\partial y_*}\right)_w, \tag{23}$$

$$\left(\frac{\partial C_*}{\partial y_*}\right)_f = Rd\left(\frac{\partial C_*}{\partial y_*}\right)_w \tag{24}$$

where $Rc = k_w/k$ and $Rd = \rho_w D_w/\rho_0 D$ are the heat and mass transfer mass diffusion coefficient ratios between the material of the separating walls and the medium that fills the cavity.

To close the problem, it is assumed to be a vertical stack of equal cavities, with the same conditions in each two adjacent cavities, thus leading to a periodic boundary condition over the y_* direction. It can then be written that

$$T_*(x_*, 1 + B/2L) = T_*(x_*, -B/2L);$$

$$C_*(x_*, 1 + B/2L) = C_*(x_*, -B/2L). \tag{25}$$

Even if the spatial periodicity is always maintained, the foregoing boundary conditions cannot be used in the case of an adiabatic or/and impermeable wall, situation that requires, over the interfaces, $(\partial T_*/\partial y_*)_f = 0$ or/and $(\partial C_*/\partial y_*)_f = 0$, respectively, being two adjacent cavities not linked by heat or/and mass transfer in this case.

2.5. *Heat and mass transfer rates*

In order to evaluate the local and global heat and mass transfer rates, one begins defining, respectively, the local Nusselt and Sherwood numbers, referred to the pure conduction situation through the medium that fills the cavity, at each point P of the wall–fluid interface, as

$$Nu_P = \frac{-k(\partial T/\partial n)_P}{k(T_H - T_C)/L} = -\left(\frac{\partial T_*}{\partial n_*}\right)_{P_*}, \tag{26}$$

$$Sh_P = \frac{-\rho_0 D(\partial C/\partial n)_P}{\rho_0 D(C_H - C_C)/L} = -\left(\frac{\partial C_*}{\partial n_*}\right)_{P_*} \tag{27}$$

where n_* is the dimensionless inward normal direction to the wall under analysis. A positive local Nusselt number means that there is a heat inflow to the cavity at P and heat outflow otherwise; the same is also valid for the local Sherwood number.

The overall Nusselt and Sherwood numbers, corresponding to each overall interface, can be obtained by integrating the foregoing local expressions. However, when analysing the overall heat and mass transfer crossing the cavity, including its diffusive separating half walls, one should also consider the transfers occurring along these walls. For a complete cavity, including two top and bottom half walls, one can consider corrected Nusselt and Sherwood numbers over each vertical wall, which include the diffusion occurring along these half walls. Locally, equations (26) and (27) are thus applied over the upper and bottom half walls as $Nu_P = -Rc(\partial T_*/\partial n_*)_{P_*}$ and $Sh_P = -Rd(\partial C_*/\partial n_*)_{P_*}$. The vertical global Nusselt and Sherwood numbers are thus obtained by integrating over the overall vertical walls, including the two half walls.

2.6. *Numerical modelling*

The set of differential equations [equations (6)–(12)] is solved by the SIMPLER method of Patankar [16], using backward staggered grids for the velocity components, and integrating the convection–diffusion terms by using the power law scheme. This is an iterative scheme, in which the estimated velocities are corrected with pressure correction terms in order to satisfy the integral continuity equation, being the pressure field directly obtained in each iteration by solving its discretization equations set. The discretization equations, formally the same for all variables, are solved iteratively with the tri-diagonal matrix algorithm (TDMA) applied several times over a complete line in each direction. On the y_* direction, the spatially periodic boundary conditions given by equation (25) are applied by using a cyclic version of the TDMA algorithm. Over the fluid–solid interface, the conjugated combined heat and mass transfer problem is solved through the use of the harmonic mean practice for the diffusion coefficients, as proposed by Patankar [16].

The domain is discretized using a 51×53 non-uniform grid, which is symmetric relative to the centre of the cavity and expands from the wall to the centre with an expansion factor of 1.08. There are considered two horizontal rows of nodes over each half solid wall. The used grid was selected from the analysis of some

preliminary tests of asymptotic type, and comparisons with the benchmark solution of Davis [17] for the single natural convection heat transfer in a square enclosure. The iterative process is stopped when the residual's summation of the momentum equations in each co-ordinate direction, normalised with $Ra_T(1+N)$, is less than 5×10^{-7}.

3. RESULTS AND ANALYSIS

3.1. *Values for the dimensionless parameters*

The dimensionless parameters governing the conjugated combined heat and mass transfer problem are seven, as shown in the preceding section: Pr, Ra_T, N, L/B, Le, Rc and Rd. There is also the possibility of T_H and C_H at the same vertical wall (combined buoyancy effects) or on the opposite vertical walls (opposed buoyancy effects).

If the medium that fills the cavity is the moist air, with a low concentration of water vapour, one can take $Pr = 0.7$ and $Le = 0.8$ (which gives $Sc = 0.6$). In order to obtain a contained work, the results are restricted to a cavity with $L/B = 20$. For the moist air $(M_2 - M_1) > 0$, being thus $\beta_C > 0$ and, consequently, $N \geqslant 0$. This last parameter is null for the situation of no solutal diffusion.

The representative results are obtained for $Ra_T = 10^5$, the remaining dimensionless parameters being grouped in order to show that the influence of the participating walls cannot be neglected in many usual situations where it is usually neglected. All the considered situations are for $Rc \geqslant Rd$, which is the most usual case for building elements.

It should be noted that the obtained results must be used with great care, due to the real possibility of the non-considered condensation of the diffusing species. Using the knowledge of psycrometry, and noting that C is the specific humidity in a wet basis, one can construct Fig. 2, where under the curve is shown the region of real validity of the obtained results for the moist air over a given range of temperature level. Similar figures can be obtained to other gaseous mixtures, the special need being the knowledge of the functional relation between the temperature and the vapour pressure of the diffusing species.

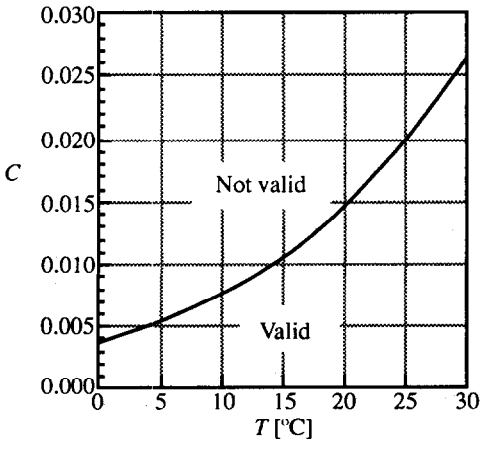

Fig. 2. Validity of the obtained results for moist air.

3.2. *Heatlines and masslines*

The heatlines and masslines are the best choice to visualise the paths followed by the heat and mass flows that cross the cavity. Such lines are defined, respectively, as the constant lines of the heat (H) and mass (M) functions, defined through its first derivatives. For the medium that fills the cavity we have

$$\frac{\partial H}{\partial y} = \rho_0 u c_p (T - T_C) - k\frac{\partial T}{\partial x};$$

$$-\frac{\partial H}{\partial x} = \rho_0 v c_p (T - T_C) - k\frac{\partial T}{\partial y}, \tag{28}$$

$$\frac{\partial M}{\partial y} = \rho_0 u (C - C_C) - \rho_0 D\frac{\partial C}{\partial x};$$

$$-\frac{\partial M}{\partial x} = \rho_0 v (C - C_C) - \rho_0 D\frac{\partial C}{\partial y}. \tag{29}$$

The corresponding equations over the separating solid walls are

$$\frac{\partial H}{\partial y} = -k_w\frac{\partial T}{\partial x}; \quad -\frac{\partial H}{\partial x} = -k_w\frac{\partial T}{\partial y}, \tag{30}$$

$$\frac{\partial M}{\partial y} = -\rho_w D_w\frac{\partial C}{\partial x}; \quad -\frac{\partial M}{\partial x} = -\rho_w D_w\frac{\partial C}{\partial y}. \tag{31}$$

The statement of the equality of the second order cross derivatives of H and M leads, identically, to the dimensional forms of equations (9)–(12).

The differential equations from which are evaluated the H and M fields are obtained by setting the equality of the second order cross derivatives of T and C from equations (28)–(31). Defining the dimensionless heat and mass functions, respectively, as

$$H_* = H/k(T_H - T_C), \tag{32}$$

$$M_* = M/\rho_0 D(C_H - C_C)Le \tag{33}$$

one obtains, for the medium that fills the cavity,

$$0 = \frac{\partial^2 H_*}{\partial x_*^2} + \frac{\partial^2 H_*}{\partial y_*^2} + \frac{\partial}{\partial x_*}(v_* T_*) - \frac{\partial}{\partial y_*}(u_* T_*), \tag{34}$$

$$0 = \frac{\partial^2 M_*}{\partial x_*^2} + \frac{\partial^2 M_*}{\partial y_*^2} + \frac{\partial}{\partial x_*}(v_* C_*) - \frac{\partial}{\partial y_*}(u_* C_*). \tag{35}$$

These equations are also valid over the solid walls, noting that, in that case, $u_* = v_* = 0$.

The H_* and M_* fields are defined through its first order derivatives, being thus important only differences in its values but not its level. This relative nature is similar to that of the pressure field in incompressible fluid flows. We have thus the freedom to state that $H_*(0,0) = M_*(0,0) = 0$. As the difference between the values of H_* and M_* at two points represents (by unit depth), respectively, the dimensionless heat and

mass flow within the two points (the later divided by Le), the boundary conditions for equations (34) and (35) are [18]:

Over the vertical walls, at $x_* = 0$ and $x_* = 1$,

$$H_*(x_*, y_*) = H_*(x_*, 0) + \int_0^{y_*} -Rc\left(\frac{\partial T_*}{\partial x_*}\right) dy_*, \quad (36)$$

$$M_*(x_*, y_*) = M_*(x_*, 0) + \int_0^{y_*} -\frac{Rd}{Le}\left(\frac{\partial C_*}{\partial x_*}\right) dy_* \quad (37)$$

noting that $Rc = Rd = 1$ for $0 < y_* < 1$.

Over the top and bottom half separating walls considered, at $y_* = -B/2L$ and $y_* = +B/2L$,

$$H_*(x_*, y_*) = H_*(0, y_*) - \int_0^{x_*} -Rc\left(\frac{\partial T_*}{\partial y_*}\right) dx_*, \quad (38)$$

$$M_*(x_*, y_*) = M_*(0, y_*) - \int_0^{x_*} -\frac{Rd}{Le}\left(\frac{\partial C_*}{\partial y_*}\right) dx_*. \quad (39)$$

The heat and mass functions are evaluated only for visualization purposes, once known the flow, temperature and concentration fields, using the calculation method proposed by Patankar [16] for conduction-type problems. The solid–fluid interfaces are treated using once again the harmonic mean practice for the diffusivities, noting that the *diffusion coefficients* for H_* and M_* are, respectively, 1 and $1/Le$ over the medium that fills the cavity, and $1/Rc$ and Le/Rc over the half solid walls.

3.3. *Temperature and concentration fields and heat and mass transfer parameters*

For comparison purposes, the presentation of results starts in Fig. 3 with the situations of no solute transfer ($N = 0$), and $Rc = 0$ or $Rc = 1$. For $Rc = 10$, the results are essentially the same as for $Rc = 1$, which are thus not presented. For $N = 0$ and $Rc = 0$ [Fig. 3(a)] we have the celebrated problem of natural convection in a square enclosure. It is observed that the temperature and heat function contour maps change markedly when Rc changes from 0 to 1, only minor changes being observed in such contour plots when Rc changes from 1 to 10. The thermal stratification at the centre of the cavity is loosed when $Rc = 1$ or $Rc = 10$, with a x_* increasing temperature profile in that region. The diffusive walls enable the heat transfer between adjacent cavities, increasing such heat exchange as Rc increases. This point is illustrated with the heatlines crossing the horizontal walls. The local and global Nusselt numbers corresponding to the vertical walls change considerably when Rc changes from 0 to 1, the global Nusselt number decreasing as Rc increases. The distribution of the local Nusselt number becomes more flat as Rc increases from 0 to 1, increasing near the upper wall and decreasing near the bottom one. It should be noted that the consideration of the heat transfer along the separating walls leads to an aforementioned *corrected* Nusselt number over such walls. Only a small increase of the global Nusselt numbers associated with the vertical walls is observed when Rc changes from 1 to 10. All the heatlines show a circulating core, with a global insulation effect over the cavity, the effective heat transfer occurring along a thin region near the top wall.

In Fig. 4 are presented the situations of combined heat and solute buoyancy effects and $N = 1$, corresponding to some particular combinations of Rc and Rd. The marked change in the presented situations occurs when Rc and Rd change from 0 to 1, only minor changes being observed when Rc and/or Rd increase from 1 to 10. This is observed from the four contour plots of temperature, concentration, heat function and mass function, and also from the Nusselt numbers. The concentration field is very close to the temperature field, $Le \approx 1$, and both the heat and masslines show to have similar behaviours for similar values of Rc and Rd. Once again, the thermal and concentration stratification at the centre of the cavity when $Rc = Rd = 0$ is replaced by x_* increasing temperature and concentration profiles. The contour plots of temperature are more inclined than these of concentration, which is due to the higher diffusion coefficient for the solute transfer, $1/Le$, with $Le < 1$. From the contour plots it is clear the extension of the temperature and concentration fields through the horizontal walls, as well as the paths followed by the heat and solute through the same walls. The influence of Rc and Rd over the Nusselt and Sherwood numbers is similar to that described (for the Nusselt number) when analysing Fig. 3, with a decrease when (Rc, Rd) change from $(0,0)$ to $(1,1)$, and a small increase when changing from $(1,1)$ to $(10,1)$ or $(10,10)$. As $Le \approx 1$, the local and global Sherwood numbers are always very close to the corresponding Nusselt numbers, this for similar values of Rc and Rd. Comparing with the situation of no solute transfer (Fig. 3), the presence of the combined buoyancy effects increases considerably the Nusselt number when $Rc = Rd = 0$. This increase is only of small significance when changing (Rc, Rd) from $(0,0)$ to any $(Rc, Rd) \neq (0,0)$.

Figure 5 represents the situations corresponding to these represented in Fig. 4, but with the buoyancy ratio $N = 10$. The major change occurs once again when changing (Rc, Rd) from $(0,0)$ to $(1,1)$, being the overall analysis made for Fig. 4 also valid for Fig. 5. However, the thermal and concentration fields shows to be more stratified, and there is a marked change over the flow structure at the centre of the cavity. In fact, it appears a region with an anti-clockwise rotation (contrary to the global one), which is more intense as Rc and/or Rd increase. The region used for the effective heat and solute transfer in the x_* direction is very close to the upper wall. The temperature and concentration contour plots for $Rc = Rd = 0$ are very close to these obtained for the single natural convection heat transfer problem with $Ra_T = 10^6$, as well as the global Nusselt number [17]. This is the expected behaviour due to the $Ra_T Pr(T_* + NC_*)$ source term in the v_* momentum equation. As expected, the Nusselt number increases

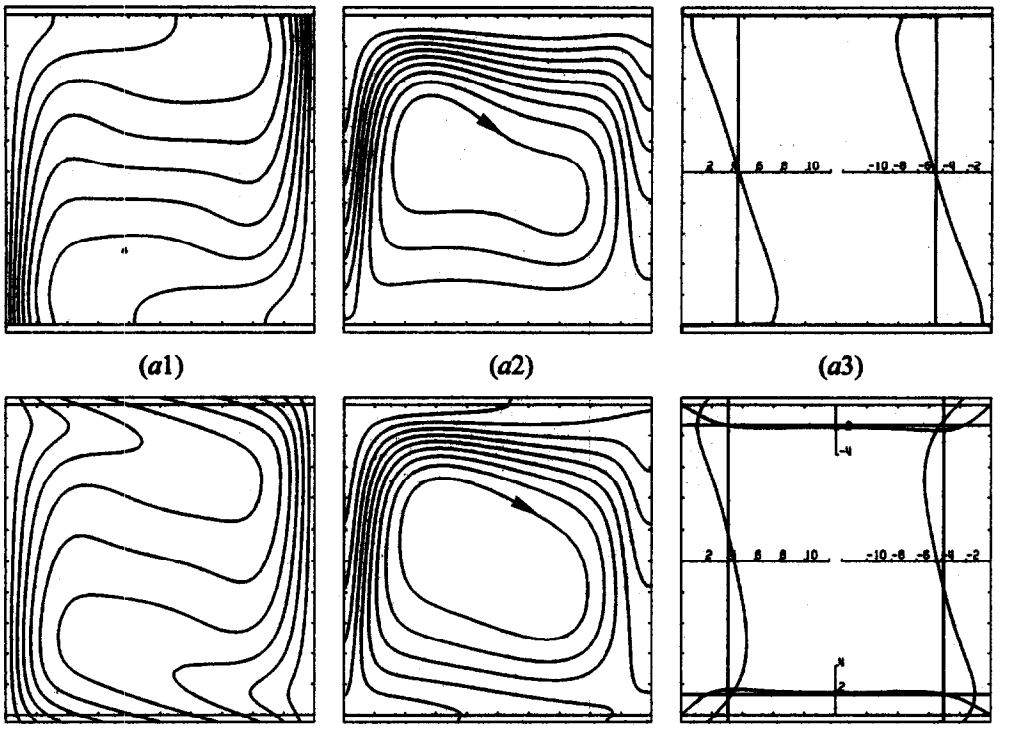

Fig. 3. Base legend as in Fig. 4. No solute transfer ($N = 0$) and: (a) $Rc = 0$ ($\Delta H_* = 0.73$); and (b) $Rc = 1$ ($\Delta H_* = 0.88$).

significantly when changing N from 1 to 10, which is a situation that is markedly controlled by the solute buoyancy effect. The effect of Rc and Rd over the local and global Nusselt and Sherwood numbers is similar to that observed when analysing Fig. 4.

For the situation of combined buoyancy effects, one concludes that only significant changes occur over the temperature and concentration fields and over the overall Nusselt and Sherwood numbers when Rc and Rd change from 0 to 1. Posterior changes increasing the diffusivity ratios are of little effect, even over the transfer parameters corresponding to the considered top and bottom half walls.

The situation of opposed buoyancy effects and $N = 1$ is only shortly discussed. It is a very delicate situation from a numerical viewpoint, because it is very sensitive to the initial conditions and to the solution's procedure used to solve the differential equations introduced by the mathematical model. Considering, for example, the initial distributions $T_* = 1 - x_*$ and $C_* = x_*$, one obtains that $T_* + NC_* = 1$, a result that is independent of x_*. Any point in the fluid is thus under the same buoyancy effect, leading to a stagnant fluid situation. The aforementioned global corrected Nusselt and Sherwood numbers for such situations are, respectively $Nu = 1 + (B/L)Rc$ and $Sh = 1 + (B/L)Rd$. Any small disturbance introduced by the initial conditions or by the solution's procedure can lead to substantially different flow structures, because it introduces differences in an expected uniform buoyancy field.

In Fig. 6 are presented some situations corresponding to the opposite buoyancy effects, with a buoyancy ratio $N = 10$, that is, situations that are controlled by the solute buoyancy effect. The temperature and concentration contour plots take the form of the mirror images corresponding to these associated with the single natural convection heat transfer problem for $Ra_T = 10^6$, as well as the global Nusselt number [17]. There is a considerable thermal and solute stratification at the centre of the cavity. Posterior changes in (Rc, Rd) from (0, 0) lead to marked changes in the temperature and concentration contour plots. As for the combined buoyancy effects situations analysed, the solute stratification is more intense than the thermal one. A drastic change occurs over the heat and masslines, presenting now an anti-clockwise rotation. Heat flows now in the x_* direction through the region close to the bottom wall. In the combined buoyancy effects situations, heat flows from one cavity to its upper neighbour, being this flow inverted when we have the opposed buoyancy effects. The solute flowing in the x_* direction proceeds now from right to left, and flows over the narrow region close to the upper wall. Similarly to what happens in Fig. 5, there is a circulation region at the centre of the cavity (contrary to this of the main flow), which significance increases as Rc and/or Rd increase. The global Nusselt and Sherwood numbers are similar to these corresponding to the situations of combined buoyancy effects, with $N = 10$ and the same (Rc, Rd) values. However, as the main circulation was changed

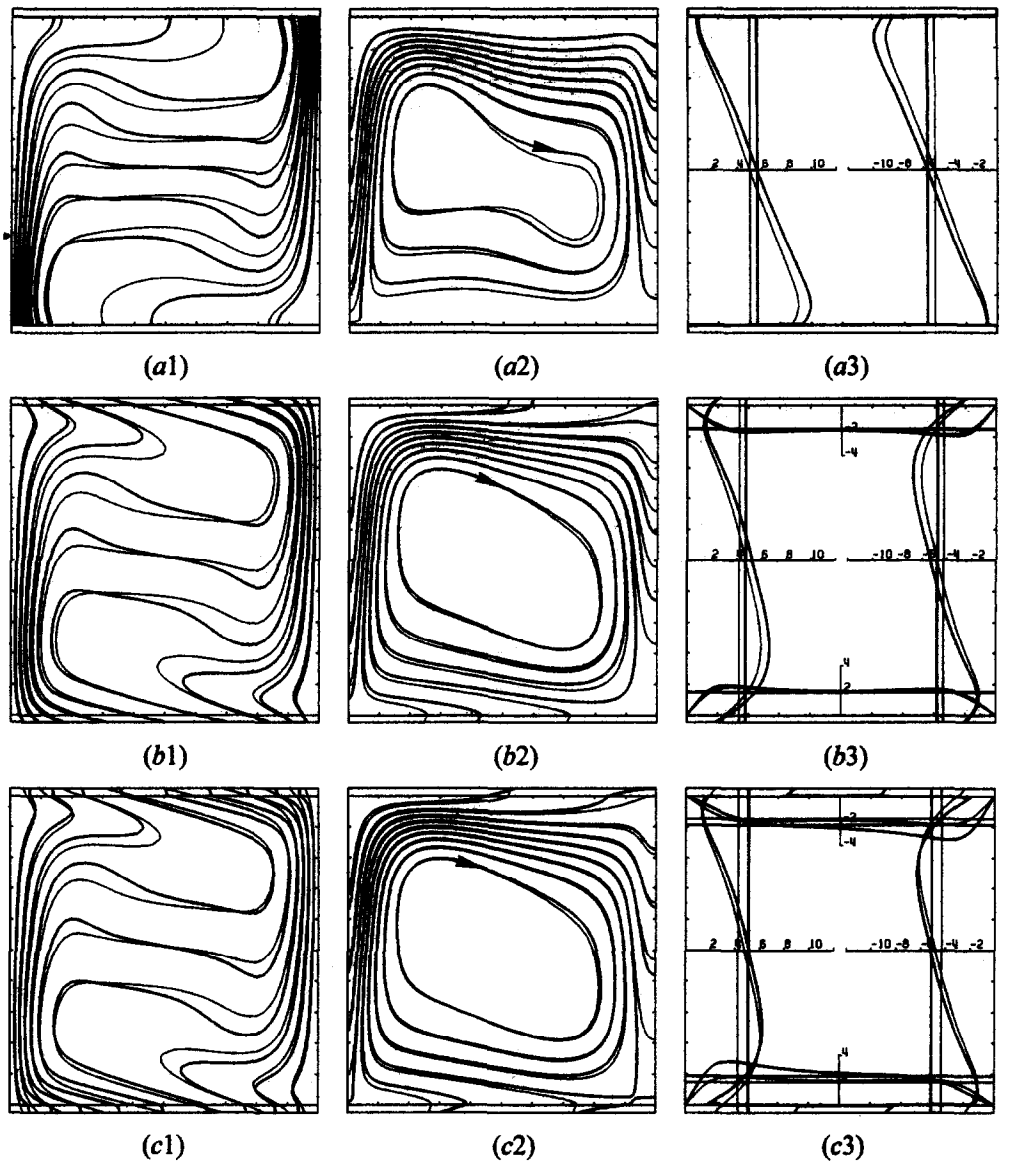

Fig. 4. Contour maps of temperature (—) and concentration (—) in (1); contour maps of heat function (—) and mass function (—) in (2); and local and global Nusselt (—) and Sherwood (—) numbers over the surfaces of the square enclosure in (3). All the contour maps in (1) with $\Delta T_* = \Delta C_* = 0.1$, being the values of ΔH_* and ΔM_* in (2) presented individually. Considered parameters are $Ra_T = 10^5$, $L/B = 20$, $Pr = 0.7$ and $Le = 0.8$. Combined buoyancy effects with $N = 1$ and: (a) $(Rc, Rd) = (0, 0)$ $(\Delta H_* = 0.92, \Delta M_* = 0.97)$; (b) $(Rc, Rd) = (1, 1)$ $(\Delta H_* = 1.11, \Delta M_* = 1.17)$; and (c) $(Rc, Rd) = (10, 1)$ $(\Delta H_* = 1.17, \Delta M_* = 1.19)$.

from clockwise to anti-clockwise, the distribution of the local Nusselt and Sherwood numbers is inverted.

For the situation of opposed buoyancy effects, and similarly to what happens with the situations of combined buoyancy effects, there are observed significant changes over the temperature and concentration fields and over the heat and mass transfer parameters when Rc and/or Rd change from 0 to 1. Only small effects are observed for changes of Rc and/or Rd from 1 to 10.

All the presented figures from Fig. 3 to Fig. 6 present a *mirror characteristic*. Each temperature and concentration contour map, each heat and mass function contour map, and each figure with the heat and mass transfer parameters exhibits this mirror characteristic: the similar image is obtained after each 180° rotation of the figure. Additionally, the temperature and concentration contour maps for the opposed buoyancy effects are, in form, the mirror images of the corresponding situations with combined heat and mass buoyancy effects.

4. CONCLUSIONS

With this work it is established the complete mathematical and numerical models for the calculation of

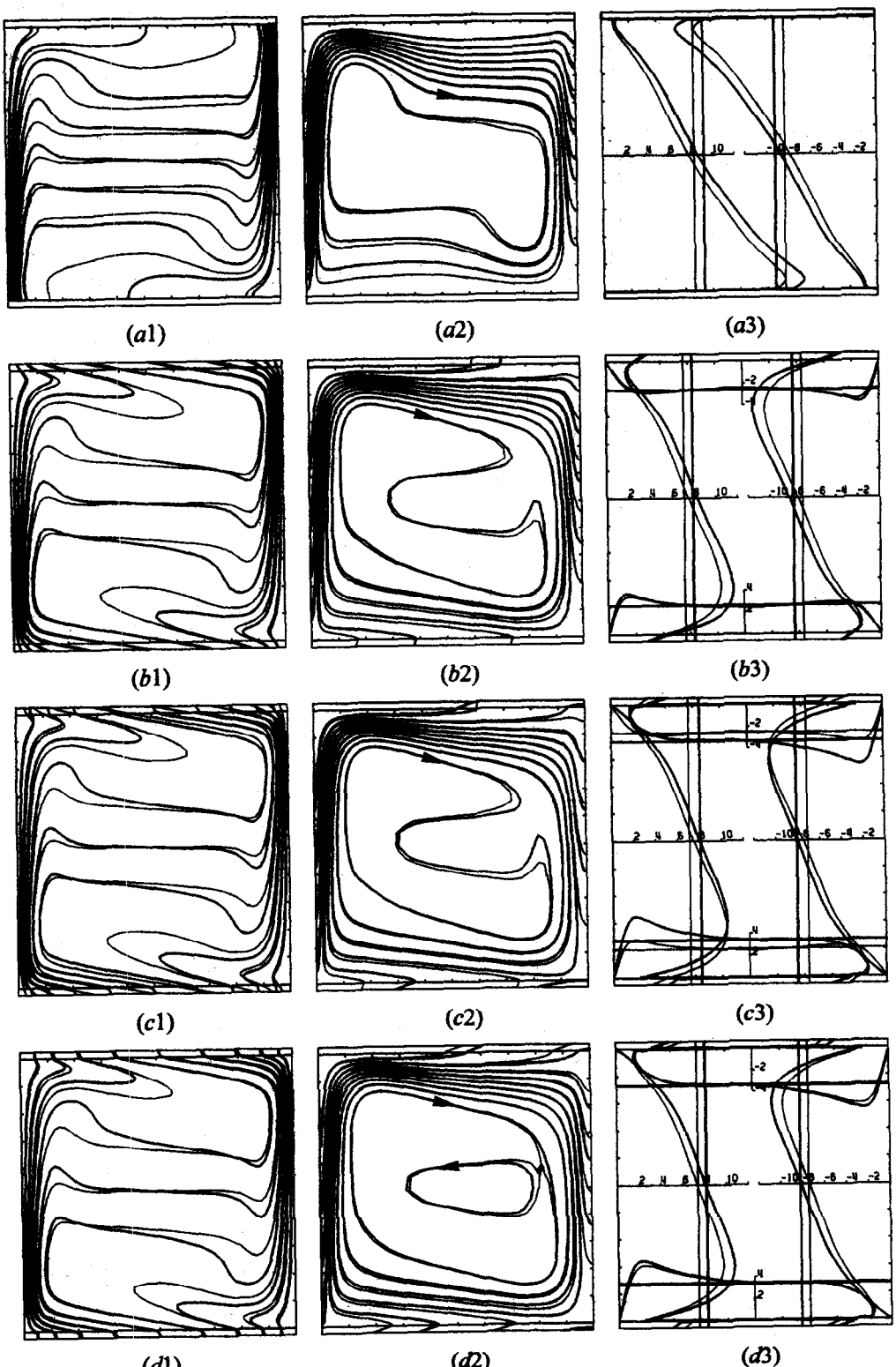

Fig. 5. Base legend as in Fig. 4. Combined buoyancy effects with $N = 10$ and: (a) $(Rc, Rd) = (0, 0)$ $(\Delta H_* = 1.47, \Delta M_* = 1.54)$; (b) $(Rc, Rd) = (1, 1)$ $(\Delta H_* = 1.78, \Delta M_* = 1.87)$; and (c) $(Rc, Rd) = (10, 1)$ $(\Delta H_* = 1.84, \Delta M_* = 1.88)$; and (d) $(Rc, Rd) = (10, 10)$ $(\Delta H_* = 1.91, \Delta M_* = 2.01)$.

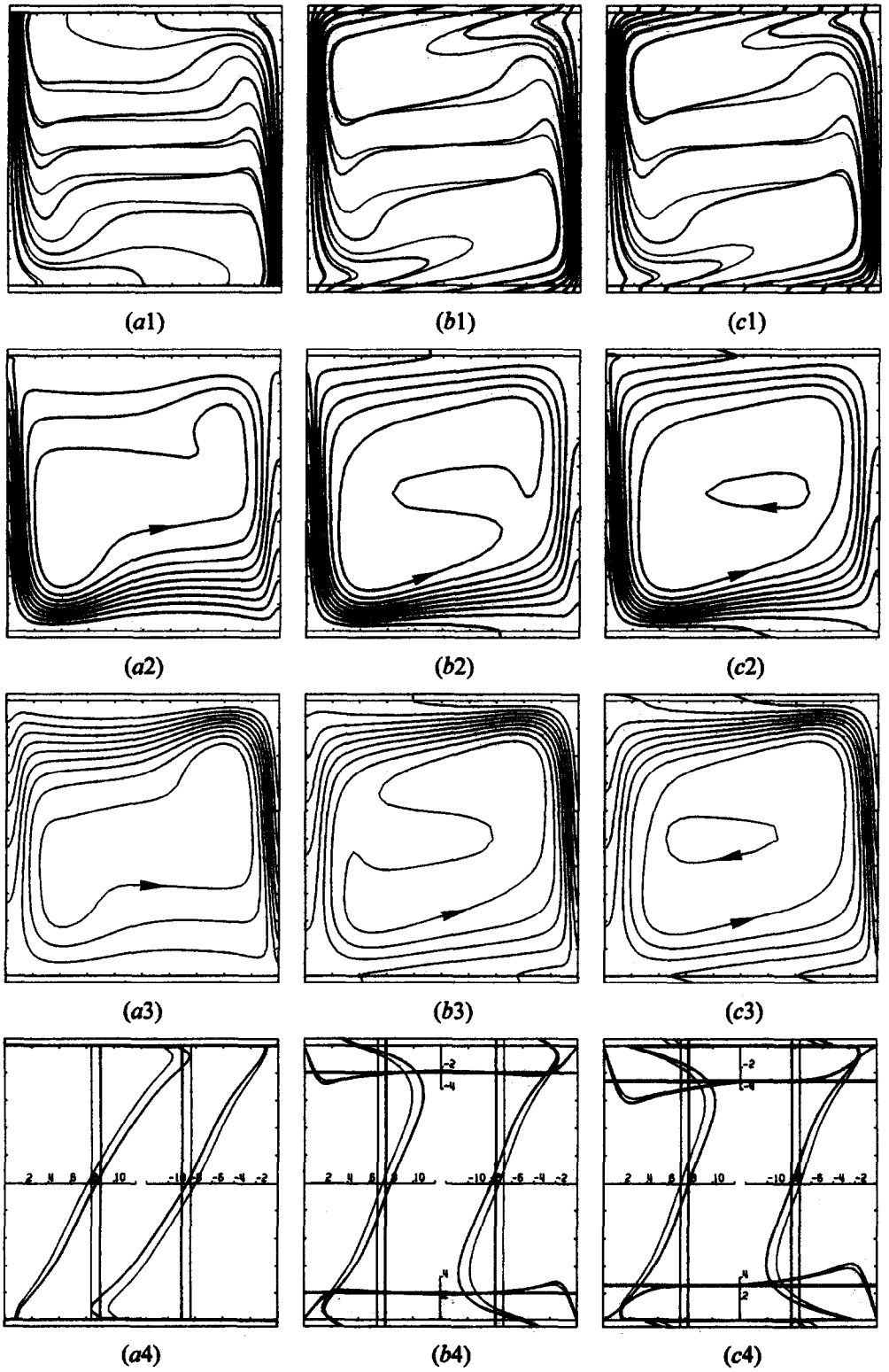

Fig. 6. Base legend as in Fig. 4, with: contour maps of temperature and concentration in (1); contour maps of heat function in (2); contour maps of mass function in (3); and local and global Nusselt and Sherwood numbers over the surfaces of the square enclosure in (4). Over the vertical walls in (4) are presented Nu and $-Sh$, and over the horizontal walls are presented $-Nu$ and Sh. Opposed buoyancy effects with $N = 10$ and: (a) $(Rc, Rd) = (0, 0)$ $(\Delta H_* = 1.45, \Delta M_* = 1.50)$; (b) $(Rc, Rd) = (1, 1)$ $(\Delta H_* = 1.72, \Delta M_* = 1.81)$; and (c) $(Rc, Rd) = (10, 10)$ $(\Delta H_* = 1.85, \Delta M_* = 1.94)$.

double diffusive natural convection in enclosures with heat and mass diffusive walls. The considerable number of involved parameters, together with the possibility of combined or opposed buoyancy effects, is a severe limitation for a much more complete analysis. A set of so many dimensionless parameters precludes the finding of general correlations for the heat and mass transfer parameters. This number is reduced in this work, by considering the moist air as the medium that fills the square cavity with a fixed L/B ratio and $Ra_T = 10^5$.

Changes on the N parameter are shown to affect seriously the temperature and concentration fields, the paths followed by the heat and mass flows, and also the heat and mass transfer parameters. By this turn, Rc and Rd diffusivity ratios affect significantly the same fields, paths and parameters when changing from 0 to 1, being the observed changes of little significance when the diffusivity ratios change from 1 to 10. The usual results obtained for the double diffusive natural convection in enclosures, of adiabatic and impermeable horizontal separating walls, are thus of little practical applicability when analysing building elements of cellular-cavity type. Special emphasis should be placed in adequate insulation for both the heat and solute, and not only on the thermal insulation, as well as in the levels of temperature and concentration within the cavities, which can lead to condensation situations. The solute buoyancy effect can very well control the natural convection in a device designed only for a good thermal insulation.

The obtained heat and masslines, for the conjugated heat and mass transfer problem under analysis are shown to be a very effective way to visualise the paths followed by heat and mass, through each cavity and also through the diffusive separating horizontal walls. Also the obtained figures with the heat and mass transfer parameters are of considerable value, giving the parameters distribution over each wall of the cavity, and also the overall parameters associated with each entire wall.

Due to the high number of involved dimensionless parameters, the main conclusion for practical purposes is that each particular case under analysis should be submitted to a complete numerical simulation, being the published results for adiabatic and/or impermeable separating walls of limited practical value.

REFERENCES

1. Kamotani, Y., Wang, L. W., Ostrach, S. and Jiang, H. D., Experimental study of natural convection in shallow enclosures with horizontal temperature and concentration gradients. *International Journal of Heat and Mass Transfer*, 1985, **28**, 165–173.
2. Kamakura, K. and Ozoe, H., Experimental and numerical analysis of double diffusive natural convection heated and cooled from opposing vertical walls with an initial condition for a vertically linear concentration gradient. *International Journal of Heat and Mass Transfer*, 1993, **36**, 2125–2134.
3. Wee, H. K., Keey, R. B. and Cunningham, M. J., Heat and moisture transfer by natural convection in a rectangular cavity. *International Journal of Heat and Mass Transfer*, 1989, **32**, 1765–1778.
4. Béghein, C., Haghighat, F. and Allard, F., Numerical study of double-diffusive natural convection in a square cavity. *International Journal of Heat and Mass Transfer*, 1992, **35**, 833–846.
5. Trevisan, O. V. and Bejan, A., Combined heat and mass transfer by natural convection in a vertical enclosure. *ASME Journal of Heat Transfer*, 1987, **109**, 104–112.
6. Nilson, R. H. and Baer, M. R., Double-diffusive counterbuoyant boundary layer in laminar natural convection. *International Journal of Heat and Mass Transfer*, 1982, **25**, 285–287.
7. Alavyoon, F., On natural convection in vertical porous enclosures due to prescribed fluxes of heat and mass at the vertical boundaries. *International Journal of Heat and Mass Transfer*, 1993, **36**, 2479–2498.
8. Mamou, M., Vasseur, P. and Bilgen, E., Multiple solutions for double-diffusive convection in a vertical porous enclosure. *International Journal of Heat and Mass Transfer*, 1995, **38**, 1787–1798.
9. Kim, D. M. and Viskanta, R., Effect of wall heat conduction on natural convection heat transfer in a square enclosure. *ASME Journal of Heat Transfer*, 1985, **107**, 139–146.
10. Du, Z.-G. and Bilgen, E., Coupling of wall conduction with natural convection in a rectangular enclosure. *International Journal of Heat and Mass Transfer*, 1992, **35**, 1969–1975.
11. Chung, K. C. and Trefethen, L. M., Natural convection in a vertical stack of inclined parallelogrammic cavities. *International Journal of Heat and Mass Transfer*, 1982, **25**, 277–284.
12. Nishimura, T., Nagasawa, F. and Kawamura, Y., Natural convection in horizontal enclosures with multiple partitions. *International Journal of Heat and Mass Transfer*, 1989, **32**, 1641–1647.
13. Costa, V. A. F., Figueiredo, A. R. and Oliveira, L. A. Convecção natural em cavidades paralelográmicas. *Proceedings of the I Congreso Iberoamericano de Ingeniería Mecánica*, E. T. S. Ingenieros Industriales, Madrid, Vol. 2, 1993, pp. 255–260.
14. Bejan, A., *Convection Heat Transfer*, 2nd edn. Wiley, New York, 1995, pp. 488–494.
15. Eckert, E. R. G. and Drake, R. M., *Analysis of Heat and Mass Transfer*. McGraw–Hill, New York, 1972, pp. 715–722.
16. Patankar, S. V., *Numerical Heat Transfer and Fluid Flow*. Hemisphere/McGraw–Hill, Washington, DC, 1980.
17. de Vahl Davis, G., Natural convection of air in a square cavity: a bench mark numerical solution. *International Journal for Numerical Methods on Fluids*, 1983, **3**, 249–264.
18. Bello-Ochende, F. L., A heat function formulation for thermal convection in a square cavity. *International Communications in Heat and Mass Transfer*, 1988, **15**, 193–202.